
Intelligent Router for LLM Workloads: Improving Performance Through Workload-Aware Scheduling

Kunal Jain Anjaly Parayil Ankur Mallick Esha Choukse Xiaoting Qin

Jue Zhang Íñigo Goiri Rujia Wang Chetan Bansal Victor Rühle

Anoop Kulkarni Steve Kofsky Saravan Rajmohan

{t-kunjain, aparayil, ankurmалlick, esha.choukse,
xiaotingqin, jue.zhang, inigog, rujiawang, chetanb, virueh,
anoop.kulkarni, stephenk, saravan.rajmohan}@microsoft.com

Abstract

Large Language Model (LLM) workloads have distinct prefill and decode phases with different compute and memory requirements which should ideally be accounted for when scheduling input queries across different LLM instances in a cluster. However existing scheduling algorithms treat LLM workloads as monolithic jobs without considering the distinct characteristics of the two phases in each workload. This leads to sub-optimal scheduling and increased response latency. In this work, we propose a heuristic-guided reinforcement learning-based intelligent router for data-driven and workload-aware scheduling. Our router leverages a trainable response-length predictor, and a novel formulation for estimating the impact of mixing different workloads to schedule queries across LLM instances and achieve over 11% lower end-to-end latency than existing approaches.

1 Introduction

The emergence of large language models (LLMs) and their generative ability has led to an increase in their usage in conversational engines, search engines, and code assistants Chen et al. [2021], Adiwardana et al. [2020], Roller et al. [2020]. The widespread usage of these large models, coupled with the significant GPU compute required for inference, has made LLM inference the dominant GPU workload. Optimizing LLM inference is thus critical for improving user experience, lowering the pressure on GPU resources, and reducing the environmental impact of running LLM workloads, and so there has been a flurry of recent work looking at various aspects of LLM inference optimization Zhang et al. [2024], Spector and Re [2023], Li et al. [2024], Lin et al. [2024].

LLM inference is usually performed on the cloud by model instances hosted by commercial cloud providers [Microsoft, Google] or dedicated LLM inference platforms [HuggingFace, OpenAI] that serve inference requests from a variety of tenants. Owing to the widespread use of LLMs in chats, document summarization, and content creation, the requests vary in terms of their input and output characteristics. Each LLM instance that serves the inference request contains a scheduler, which is a batching system responsible for creating a batch of requests by retrieving requests from a queue and scheduling the execution engine. There exist multiple approaches in the literature that try to optimize the batching of these requests at the LLM instance level [Yu et al., 2022, Patel et al., 2023,

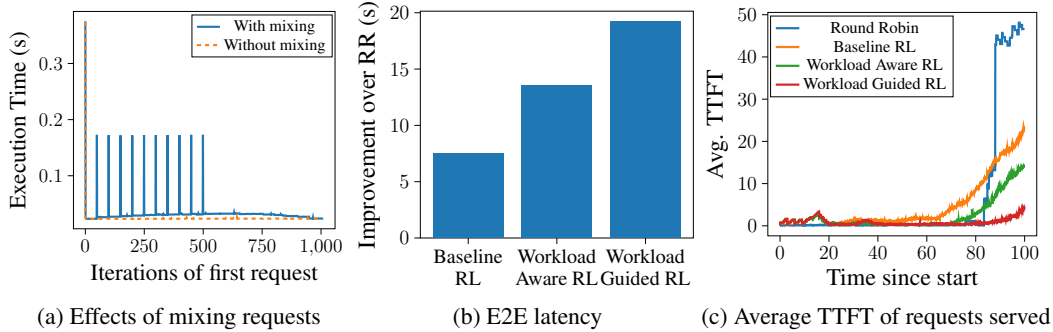


Figure 1: Key Results: (a) Spikes in the blue plot corresponds to prompt (input processing) phase of incoming requests due to which the total execution time of the original request will be much higher (see section 4). (b) Our RL-based approaches improve upon Round-robin (RR) routing in terms of overall latency with Workload Guided RL reducing average end-to-end latency by 19.18 seconds. (c) The average Time-To-First-Token is the lowest for the proposed approach.

Agrawal et al., 2024, Zhong et al., 2024] with various goals like reducing queuing delay of requests, maximizing the utilization of the serving infrastructure, etc.

While each of these approaches has its own strengths and weaknesses, this literature has so far lacked an investigation of *techniques for routing requests across multiple LLM instances*. This is a significant gap since the wide variety in the size of input queries and LLM responses across scenarios implies that sub-optimal request assignment can significantly increase inference latency. Figure 1a shows spikes in execution time of a request when new requests are added while the LLM instance is processing an initial request. Thus, even the performance of an optimal scheduler at the LLM model instance depends crucially on the assignment of requests to instances. Figure 2 shows another task which empirically explains the effect of mixing requests: if you have 8 requests coming in of random lengths at intervals of one second each and 2 model instances, what is best, average and worst way to assign 4 requests to each model? When we vary the request lengths from 10 to 1000 prompts and decode tokens, we see that while the average latency for processing in our set up is 29.81 seconds, the best achievable latency is 27.03 seconds and the worst can go upto 32.34 seconds. This means that a random assignment, on average, yields 10% higher end-to-end latency than the optimal

In this work, we demonstrate that serving inference requests with diverse characteristics concurrently on a model instance negatively impacts end-to-end latency. We develop a lightweight decode length predictor and by classifying requests based on prompt and decode characteristics, we model the latency impact of mixing incoming and existing requests. The proposed approach is extensible to any new hardware and model pairs, as the latency impact estimator utilizes profiling information from the underlying model and hardware pair. Finally, we leverage the proposed models for output length prediction and the latency impact of mixing requests to propose a workload-aware, reinforcement learning-based router. This router assigns requests to one of the available model instances to minimize end-to-end latency. Our approach reduces queuing at model instances as compared to current routing schemes that ignore variations in the input and output characteristics of workloads. This improves latency by 11.43% on average for 2000 requests over 4 LLM instances. This is achieved by strategically delaying routing and selecting the best model instance based on the current state of LLM instances and incoming requests.

Contributions. Firstly, we established the impact of concurrently serving inference requests with diverse characteristics (section 4). Secondly, we proposed a novel formulation to model this impact(section 4). Thirdly, we developed a lightweight model for predicting decode length, performing well across various prompt and decode characteristics (subsection 5.1). Lastly, we proposed a heuristic-guided, workload-aware reinforcement learning router that encodes prior knowledge of workload mixing effects, achieving improved end-to-end performance (subsection 5.3).

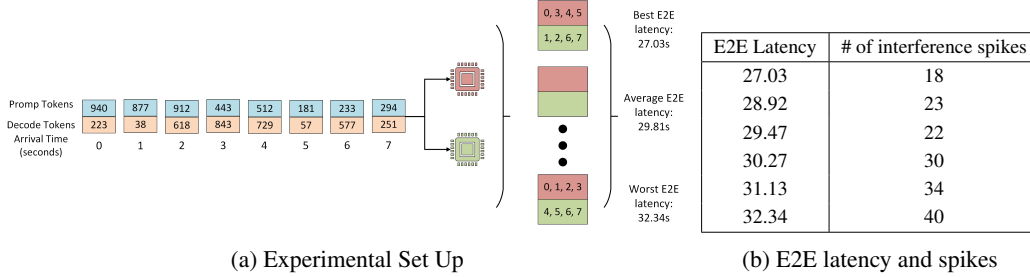


Figure 2: (a) We take 8 requests of random shapes coming in at intervals of 1 second. Each of these requests can be routed to one of two identical model instances. After a complete search over all the possible ways to route these requests between the two models, we find that the best possible end-to-end latency for processing all eight requests is 27.03 seconds, while the worst is 32.34 seconds. If we do random assignment, we get an expected latency of 29.81 seconds, showcasing that the ideal case is about 10% better than the average in this small example. (b) This shows us the correlation between the spikes observed during inference because of mixing prompt and decode phases and the E2E latency. We notice that the number of spikes is substantially more than the number of requests due to request preemption, which forces the prompt to be processed again.

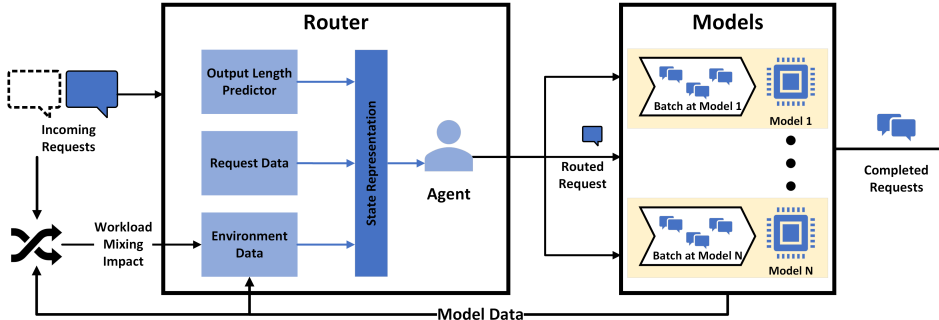


Figure 3: Our intelligent router uses the output length predictor and workload impact estimator to inform decision-making. It routes incoming requests to the appropriate model instance based on request characteristics and the state of the instances. On the other hand current approaches focus on instance-level scheduling shown by highlighted regions around each model instance.

2 Preliminaries

LLM requests. Large Language Models (LLMs) go through prompt/prefill and decode phases while serving a request. The prefill phase processes input tokens in parallel performing self attention computations at each layer and is thus typically compute bound. The decode phase generates subsequent output tokens sequentially based on the forward pass of the last output token and cached context (\mathbf{K} and \mathbf{V} matrices) from previous tokens and is thus memory bound Agrawal et al. [2023]. The response generation ends either when the model produces an EOS token or if the request reaches its maximum token count. A single forward pass of the model is referred to as one iteration of the model Yu et al. [2022].

Scheduler block at LLM instance. Each LLM instance that serves the inference request contains a scheduler, which is a batching system responsible for creating a batch of requests by retrieving requests from a queue and scheduling the execution engine. The scheduler controls how many and which requests are processed in each iteration and may use techniques like iteration-level scheduling introduced in Yu et al. [2022] to reduce queuing delay. The highlighted blocks in Figure 3 show the scheduler at each LLM instance. Often, the First-Come-First-Served policy is used for scheduling requests as the online requests are latency-sensitive.

LLM Output length prediction. Prior works such as S^3 [Jin et al., 2023] also focus on optimizing the throughput of the LLM instance by predicting the output sequence length given an input prompt

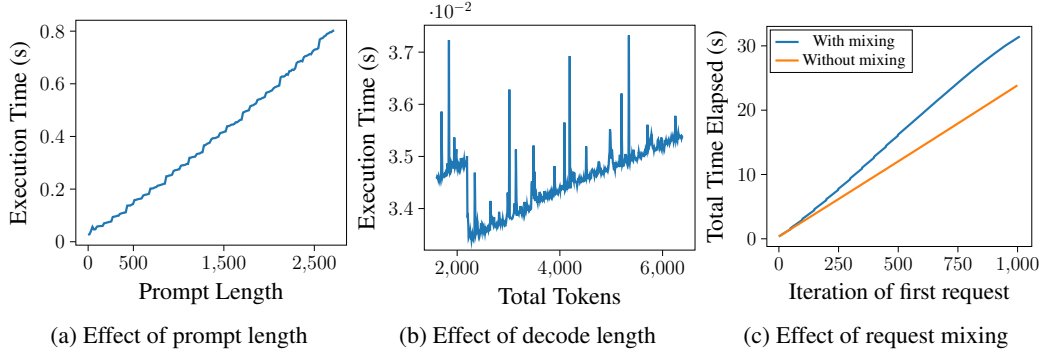


Figure 4: **Effects of prompt and decode tokens on batch execution time.** (a) Execution time of batch with a request in prefill phase grows fast and linearly with the number of prefill tokens. (b) Execution time of batch with only decode tokens is affected to a much lesser degree with the number of tokens. (c) Increase in execution time on mixing requests with the arrival pattern of Figure 1a

using a lightweight Distilbert model and batching inputs based on the predicted output length. The prediction is treated as a classification problem by dividing output length into 10 uniform buckets and training the predictor to pick the correct bucket for an input. This lightweight approach predicts output length with 98.6% accuracy on a QnA dataset and we build on it in this work.

Problem Setup. We consider serving a stream of requests using multiple homogeneous LLM instances, each with a scheduler Yu et al. [2022] to iteratively batch requests using a First-Come-First-Served policy. Requests vary in tasks like summarization, QnA, and translation, each with different prompt and decode characteristics. Requests queue centrally and are routed one at a time to an LLM instance with available capacity. Due to memory constraints, a request may be preempted mid-process if its response exceeds expected size. Assuming the request arrival rate maintains system equilibrium, our goal is to assign requests to LLM instances to minimize end-to-end latency.

3 Related Work

LLM Serving Systems. Recent advancements in inference serving systems for LLMs have focused on optimizing throughput, latency, and resource management. ORCA Yu et al. [2022], Sarathi Agrawal et al. [2023], FlashAttention Dao et al. [2022], and vAttention Prabhu et al. [2024] are examples of systems that have achieved significant improvements in performance through techniques such as iteration-level scheduling, innovative batching, and IO-aware algorithms.

LLM Serving Algorithms. This space has also seen several algorithmic innovations. QLM (Jha et al.) utilizes Bayesian statistics and stochastic programming to manage non-deterministic execution times inherent in LLMs. Similarly, Qiu et al. [2024] advocates for speculative shortest-job-first scheduling, and Wu et al. [2023] employs preemptive scheduling to improve performance. DistServe and Splitwise (Zhong et al. [2024], Patel et al. [2023]) optimize LLM serving performance by separating prefill and decoding computation for throughput enhancement while maintaining low latency. In addressing system load and request patterns, Jha et al. [2024] and Mendoza et al. [2024] utilize deep reinforcement learning to dynamically adjust service quality, increasing hardware utilization for cost-efficient serving. Additionally, Liu et al. [2024] optimize Quality-of-Experience (QoE) for LLM serving systems, focusing on user-centric metrics to enhance individual experiences. While these works optimize request scheduling at the instance level, they ignore the diversity in the prompt and decode characteristics across requests.

Reinforcement Learning for routing jobs. Reinforcement Learning (RL) has been a natural choice for routing jobs in multi-server queues owing to the challenges in deriving exact policies. While previous works [Staffolani et al., 2023, Jali et al., 2024] have looked at general jobs, in this work we leverage the specific characteristics of LLM requests and insights from our workload-study to design novel workload aware RL approaches for routing inference requests across LLM instances.

Source	Task	Samples	Average Tokens		Heavy Decode	Accuracy	
			Prompt	Decode		SOTA	Ours
Books Tiedemann [2012]	Translation	7351	29.09	61.76	9.18%	4.47%	93.10%
Eli5 (Reddit subset) Fan et al. [2019]	QnA	6988	29.83	334.40	58.18%	5.91%	70.36%
IMDb Maas et al. [2011]	Sentiment Analysis	6564	211.54	142.53	41.01%	6.81%	79.92%
SQuAD Rajpurkar et al. [2016]	In-context QnA	7122	125.16	220.02	47.95%	6.22%	65.27%
WNUT Derczynski et al. [2017]	Entity Recognition	3304	26.41	64.10	8.71%	2.76%	95.06%
Total	-	31329	89.03	175.71	35.54%	5.5%	79.15%

Table 1: **Dataset and Performance of Output Length Predictor.** Average prompt and decode tokens varies across data sources. The second last column indicates the percentage of requests with heavy decodes (≥ 5 seconds estimated completion time) and the last column indicates the accuracy of our decode length predictor model described in subsection 5.1 for each source.

4 Observation

Request classification based on prompt-decode characteristics. In general, LLM queries come from different tasks and differ in terms of their prompt and decode distribution. We simulate this using data from five different tasks: sentiment analysis, entity recognition, in-context QnA, general QnA, and translation (prompt details in Appendix A.3). Table 1 summarizes the distribution of input (prompt) and generated output (decode) tokens for the requests from these tasks. We see a clear distinction in the average length of prompt and decode tokens, and in the percentage of requests with heavy decode, across tasks.

Based on these observations, we divide requests into four categories: light prompt-light decode (LL), light prompt-heavy decode (LH), heavy prompt-light decode (HL), and heavy prompt-heavy decode (HH). Requests that take 0.5 seconds or more to complete their prompt phases are defined as heavy prompts, and requests that take 5 seconds or more in the decode phase are defined as heavy decodes. We make the division between heavy and light tokens based on latency as (i) latency is the key metric that we are optimizing in this work and (ii) they are representative of the SLAs that different service providers might have. These values are hyperparameters that can be tuned to the provider’s needs. It is to be noted that the execution time (latency) varies from one hardware to different, so in order to have a common ground, we are using prompt and decode processing time to define light/heavy classification.

Figures 4a and 4b show that batch execution time increases linearly with the number of prompt tokens due to its compute bound nature, and the growth is much slower during the decode phase. Thus, we estimate the processing time for a request with p prompt and d decode tokens as $p \times (\text{time per prompt token}) + d \times (\text{average decode batch time})$. Similarly, the earliest time any model instance will become available is $(\text{decode tokens left}) \times (\text{average decode batch time})$. In the following section, we discuss the impact of serving these requests concurrently on a single LLM instance and the effect of routing and scheduling logic on the end-to-end performance of inference across multiple model instances.

Mixing inference requests on a single model instance can harm latency and end-to-end performance. The unique characteristics of LLM requests causes the end-to-end latency to be adversely affected by continous batching of requests. For example, the ideal latency for a request with $p = 1000$ and $d = 1000$ is 17 seconds (orange plot in Figure 4c). However if we now have requests with $p = 500$ and $d = 500$ arriving and getting batched with this request at every 50th iteration then the end-to-end latency of the original request goes up to 31 seconds (Figures 1a and 4c). This is due to the latency spikes caused by the prompt phase of each of the incoming requests due to which the latency of the original request goes up even though the decoding happens in parallel. The additional latency spikes in the prompt phase differentiates LLM inference from other batch jobs.

The end-to-end latency is affected by the request arrival patterns and both the routing and the batching algorithms. To understand the effect of routing on the overall end-to-end latency of the system, we take two LLM instances and consider the following arrival patterns of 3000 requests: 1) LH and HL requests arriving in a random fashion, 2) Requests from all four classes arriving in a random fashion, 3) LH requests arriving first followed by HL requests, and 4) HL requests arriving first followed by LH requests. We study the end-to-end latency in each scenario with different

Batching Algorithm	Routing Algorithm	Total End to End Latency (seconds)			
		(LH, HL random)	(Random)	(LH, then HL)	(HL, then LH)
Bin Packing Jin et al. [2023]	Dedicated Small-Large	704.5	644.75	566.25	588.15
	Round Robin	581.5	559.3	424.8	440.68
	Decode Balancer	595.82	555.4	424.82	440.81
Least Work Left	Dedicated Small-Large	704.5	641.81	566.25	588.15
	Round Robin	585.14	554.00	424.64	440.82
	Decode Balancer	596.95	559.97	424.66	440.81
FCFS Yu et al. [2022]	Dedicated Small-Large	704.5	648.66	566.25	588.15
	Round Robin	607.45	572.16	424.80	440.82
	Decode Balancer	605.65	573.17	424.82	440.81

Table 2: **Performance of batching and routing algorithm combinations.** We simulate arrival of requests with distinct characteristics using the request classification discussed in section 4 and test the combined affect of routing and batching strategies. Good routing algorithm on an average shows greater end-to-end latency improvement compared to the batching algorithm on all the scenarios with distinct characteristics and arrival sequence.

combinations of batching and routing algorithms. Details of these algorithms are added to Appendix A.1. We can see from Table 2 that it is the combination of routing and batching algorithms that affects the overall end-to-end latency of processing the requests.

For example, the bin-packing scheduler finishes Scenario I six seconds faster when using round-robin routing compared to decode balancer routing but the same combination is four seconds slower when benchmarked on Scenario II. We also observe that sub-optimal routing strategies, such as having dedicated servers for small and large requests, can have a severely adverse effect on the overall performance of our system. This highlights the importance of optimizing the routing strategy and shows that scheduling algorithms can only provide results as good as the choices provided to it by the router.

Another interesting insight is that, for Scenario IV, all the batching algorithms show the exact same end-to-end latency, and it is the routing algorithm that improves the end-to-end latency. This is because, regardless of selecting batching algorithms such as Least Work Left, the requests coming in first have a low number of decode tokens and are thus affected less by incoming prompt tokens, which are themselves quite light. This indicates the dependence of performance on the arrival sequence of requests with different characteristics.

Insights. Quantitative analysis highlights the importance of considering request characteristics and avoiding serving requests with diverse characteristics concurrently at a single LLM instance, especially when multiple LLM instances are available. Further, the routing algorithm on an average shows greater end-to-end latency improvement compared to the batching algorithm on all the scenarios with distinct characteristics and arrival sequence. We propose to optimize routing logic for a given batching algorithm and workload characteristics. A data-driven optimal router framework can translate the improvements to any downstream batching logic. Anchoring on our thesis that batching algorithm can only provide results as good as the choices provided to it, in the next section, we propose a workload-aware intelligent router and discuss the overall design of the router and the individual building blocks required.

5 Intelligent Router: Design

Figure 3 shows the overall design of the intelligent router. Based on the insights from section 4, an intelligent router should: a) classify requests based on prompt-decode characteristics and be able to estimate decode length, b) estimate the adverse effect of mixing diverse requests at a single model instance on end-to-end latency, c) leverage prior knowledge of these adverse effects for decision making, and d) possess lightweight modules for efficient processing. To achieve this, we develop an output length predictor and workload impact estimator for intelligent routing. Additionally, we propose a reinforcement learning framework to utilize accumulated context and prior knowledge, improving end-to-end latency.

5.1 Output length predictor

Similar to [Jin et al., 2023], we generate responses for each request in the dataset discussed in section 4 and categorize each request into a bucket based on the number of output tokens in its response. We use these buckets as labels and input prompts as inputs to fine-tune a DistillBERT model for predicting the range of output tokens for new requests. However, instead of using buckets of equal size, we define the bucket ranges based on the estimated completion time for the request. Following the heavy-light decode logic described in section 4, we predict buckets with ranges 0 – 0.5 seconds, 0.5 – 0.5 × 4 seconds, 0.5 × 4 – 0.5 × 8 seconds and so forth. Our experimental set up produces roughly 500 decode tokens per second on average, to bucket sizes of 0 – 250, 250 – 1000, 1000 – 4000 and so on. Our choice of (unequal) bucket sizes helps us better distribute the requests among the buckets. This approach provides our routing strategy with actionable information by aligning the bucket ranges with the expected completion times.

We observe that the approach by Jin et al. [2023] does not directly generalize well to our dataset, which comprises requests from distinct prompt/decode distributions. The model achieves an accuracy of only 5.5% in predicting unequal-sized buckets and 9.3% in predicting equal-sized buckets of 250 tokens. Leveraging our insight from section 4 that input and output characteristics depend on the task type, we enhance the model’s performance by appending the task type as a hint to the prompt provided to the DistillBERT model. Employing this technique, we achieve an accuracy of 79.15% in predicting unequally sized buckets and 68.23% in predicting equal-sized buckets. We can predict task type from the input prompt with an accuracy of 93.79% (c.f. subsection A.6).

5.2 Workload impact estimator

Mixing requests with different prompt and decode characteristics in a model instance can impact overall latency in the following ways: (i) the latency of the incoming request during the prompt phase increases rapidly and linearly with an increase in the number of prompt tokens, and (ii) the decode phase has a much lower impact, and the mean iteration time varies slowly with an increase in total tokens. As we can see from Figure 4 (c.f. Section 3), the gradient for our configuration can be calculated as 3.2×10^{-4} and 3.3×10^{-5} . We see a roughly linear increase in batch execution with an increase in token count. The gradient is obtained by profiling the Llama-2-7b models on V100. It is to be noted that same approach can be followed to obtain the gradient for other hardware and model combination.

Let there be n requests within model instance m , and p_j^m and d_j^m indicate the number of prompt and decode tokens processed by the j -th existing request at model m . As the impact on the prompt phase is directly proportional to the number of prompt tokens in the request and the total number of tokens already running in the decode phase, we can model the impact on the prompt phase (time to process p_i , $T_{p_i}^m$) of an incoming request with p_i tokens when added to the model instance with n requests, and corresponding penalty as:

$$T_{p_i}^m = \text{grad}_1 * \left(p_i^2 + \sum_{j=1}^n (p_j^m + d_j^m) \right), \quad r_{p_i}^m = \begin{cases} 1 & \text{if } T_{p_i}^m \leq \epsilon \\ 1 - \frac{T_{p_i}^m}{\epsilon} & \text{otherwise} \end{cases}$$

Here, we introduce a penalty if the latency impact exceeds ϵ . Similarly, the impact on existing requests beyond the prompt phase is directly proportional to the total number of requests in the model. We can model the penalty due to the impact of an incoming request with p_i prompt tokens and d_i decode tokens on the decode phase of already existing n requests as:

$$r_d^m = -\text{grad}_2 * \sum_{j=1}^n (p_j^m + d_j^m) + p_i + d_i \quad (1)$$

With our selection of grad_1 as 3.2×10^{-4} and grad_2 as 3.3×10^{-5} , we expect the values r_d^m and $T_{p_i}^m$ to be in the ranges of $[-1, 1]$ and $[-1, 0]$ respectively when there are no requests waiting at the model instance. We combine subsection 5.2 and Equation 1 to get the final penalty of mixing requests: $r_{\text{mixing}}(s_t, s_{t+1}) = \alpha r_{p_i}^m + (1 - \alpha) r_d^m$ where m is the action taken for the state transition $s_t \rightarrow s_{t+1}$. Here, parameter $\alpha \in (0, 1)$ balance priority over the prompt and decode phases.

5.3 RL based Router

We formulate the problem of routing incoming requests to the m model instances as discrete-time Markov Decision Process (MDP) and propose a reinforcement learning-based solution. The discounted MDP is denoted as a tuple $\mathcal{M} = (\mathcal{S}, \mathcal{A}, P, r, \gamma)$, where \mathcal{S} is the state space, \mathcal{A} is the action space, $P(s'|s, a)$ is the transition dynamics, $r(s, a)$ is the reward function, and $\gamma \in [0, 1]$ is the discount factor. The goal is to find the policy $\pi(s|a)$, a distribution of actions over states, which maximizes the discounted return $G_t = \sum_{k=0}^{\infty} \gamma^k r_{t+k+1}$ in expectation. We assume an arrival rate of λ for the requests and the ideal estimated time to complete request i as \hat{T}_i . Let o_{jt} denote the total number of output tokens produced until time t by request j , and \hat{d}_{jt} denote the estimated decode tokens for the j -th request. Therefore, we denote the fraction of request j completed at time t by $f_{jt} := \frac{o_{jt}}{\hat{d}_{jt}}$. We assume state transition at every Δt , where Δt is the average time to generate a decode token. Next, we discuss the state space, action space, and reward setting.

State Space. At time t , the state of the system, which comprises m model instances and requests waiting in the queue, can be captured by the following: 1) The number of requests in the queue at time t , denoted by w_{qt} ; 2) The exact number of prompt tokens, denoted by $p_t \in \mathbb{R}$, and the estimated bucket for the decode tokens, denoted by $d_t \in \{0, \dots, n_d\}$, corresponding to the next request in the queue. Here, the estimated bucket varies from zero to n_d ; 3) Matrices, $\mathbf{P}_t \in \mathbb{R}^{m \times n_p}$ and $\mathbf{D}_t \in \mathbb{R}^{m \times n_d}$, capturing the prompt and decode distribution of requests at the model instances. We represent the prompt (decode) distribution by n_p (n_d) buckets. $(\mathbf{P}_t)_{i,j}$ ($(\mathbf{D}_t)_{i,j}$) denotes the number of requests in prompt (decode) phase at the i -th model instance that are present in the j -th bucket i.e. have j prompt (decode) tokens. We represent the prompt and decode distribution across the model instances as a matrix, which maintains the finite dimensionality of the state space. 4) The capacity available at the model instances at time t is denoted by $\mathbf{C}_t \in \mathbb{R}^m$, as a function $g(\text{batch size}, \mathbf{P}_t, \mathbf{D}_t)$; and 5) The estimated completion time for the earliest request in model j , denoted by \hat{T}_{c_t} .

Action Space. At any given point in time, the agent must decide whether to schedule incoming request i to any of the m model instances or choose to take no action. Therefore, $a \in \{0, \dots, m\}$.

Reward Design. Based on the insights from section 4, we include the following elements in the reward formulation: a) a negative penalty for requests in the queue, decreasing as requests are processed, to account for the autoregressive nature of requests, b) a positive reward for each completed request, and c) a workload impact estimator-based penalty, which encodes the adverse effect of routing specific requests to a model instance with existing requests, and prevents requests from being queued at each model instance due to a lack of memory. Note that adding the workload impact estimator-based penalty directly to the reward function might introduce bias. Therefore, we propose to augment the prior knowledge using a heuristic-guided formulation [Cheng et al., 2021], and the reward at time t is given by:

$$\begin{aligned} r_t &= - \sum_{j \in \mathcal{J}} \left(\frac{1}{\hat{T}_j} (1 - f_{jt}) \right) + \sum_{j=1}^m \sum_i r_w \times \mathbf{w}^{mi_t} - (\gamma - \tilde{\gamma}_k) h(\mathbf{s}_t, \mathbf{s}_{t+1}) \\ h(\mathbf{s}_t, \mathbf{s}_{t+1}) &= r_{\text{mixing}}(\mathbf{s}_t, \mathbf{s}_{t+1}) - \max_{l=1, \dots, m} (r_{\text{mixing}}(\mathbf{s}_t, \mathbf{s}_{t+1}^l)) \end{aligned} \quad (2)$$

Here, \mathcal{J} includes the set of scheduled and unscheduled requests, and $\mathbf{w}^{mi_t} \in \{0, 1\}$ indicates whether the i^{th} at the m^{th} model completed at time t . $r_w \in \mathbb{Z}^+$ is the positive reward for completing a request. The function $h : \mathbf{S} \times \mathbf{S} \rightarrow \mathbb{R}$ represents the difference in penalty due to assigning the incoming request to a model other than the one for which the impact is minimum (a function of equations subsection 5.2 and Equation 1). The term "guidance discount" is given by $\tilde{\gamma}_k = \lambda_k \gamma$, where the subscript k denotes the k -th episode. Here, $\lambda_k \in [0, 1]$ is the mixing coefficient and settles to zero with an increase in episodes [Cheng et al., 2021]. The discount factor in the MDP is set to $\tilde{\gamma}_e$ during training. The function $h(\cdot)$ returns zero when the request is assigned to the model with the least workload mixing impact. Intuitively, the formulation introduces horizon-based regularization, and its strength diminishes as the mixing coefficient increases, which modifies the original MDP, $\mathcal{M} = (\mathcal{S}, \mathcal{A}, P, r, \gamma)$, to $\tilde{\mathcal{M}} = (\mathcal{S}, \mathcal{A}, P, \tilde{r}, \tilde{\gamma})$. Over the course of training, the agent interacts with the environment, and the effects of the heuristic in the MDP decrease, and the agent eventually optimizes for the original MDP.

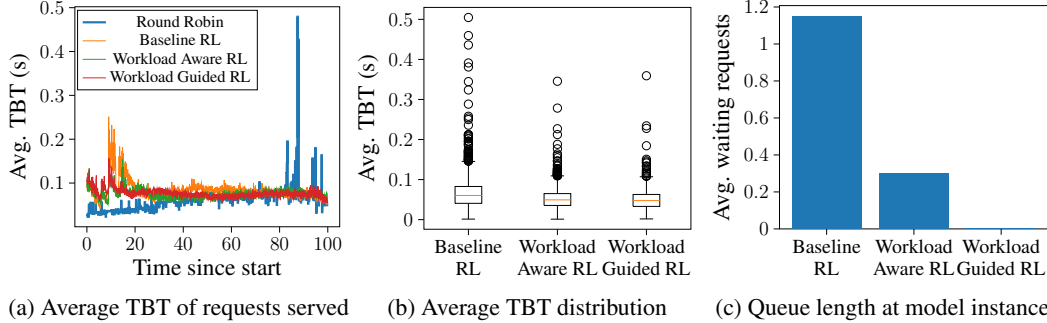


Figure 5: **Experimental Results.** We simulate the arrival of 2000 requests, each with distinct characteristics, at an arrival rate of 20 requests per second and average results over 20 episodes. Round-Robin performs better initially in terms of average TBT, but the value increases over time as more requests with different characteristics accumulate. Workload Guided RL minimizes the variance in average number of waiting requests and TBT values, with fewer requests in the waiting queue compared to other methods.

We discuss and compare results from the baseline RL formulation, results when we simply augment the penalty from r_{mixing} to the base line RL (workload knowledge augmented), and workload guided RL (heuristic guided) in section 6. Guarantees on the boundedness of the reshaped MDP’s value function directly translate from [Cheng et al., 2021].

Light-weight Heuristic. Based on our observations from section 4, we also propose a light-weight router, *earliest available model* heuristic in place of round robin, which routes a request to a model as soon as a model has enough space to serve it. While this greedily minimizes request waiting times at the router, it does not account for the requests already running at the model instance and risks getting the request preempted in the future. Overall, we observe an average improvement of 4.3 seconds (2.48%) over Round-robin using this strategy.

6 Experiments

We evaluate our methods on the dataset described in section 4 and report the end-to-end latency, Time-To-First-Token (TTFT) i.e. how quickly the user sees initial response, and Time-Between-Tokens (TBT) i.e. average token streaming latency [Patel et al., 2023] for each approach.

Setup. We route requests between 4 instances of LLama-2-7b-hf model Touvron et al. [2023] on a cluster of 4 V100 GPUs using vLLM Kwon et al. [2023] for model management with its default First-Come-First-Served (FCFS) scheduler for iteration-level scheduling. We assume an average request arrival rate of $\lambda = 20/s$, with requests uniformly sampled at random from the dataset in section 4. For consistency, we use the same set of requests across different methods during testing. The routing of requests to model instances is asynchronous, both among instances and with respect to the routing layer. Consequently, we take actions every 0.02 seconds, which we observe to be the minimum decode batch execution time. We compare the three RL approaches proposed above - Baseline RL, Workload Aware RL, and Workload Guided RL, with the Round-Robin approach.

For baseline RL, we set $\gamma - \tilde{\gamma}_e = 0$ in the reward function from Equation 2. For workload-aware RL, we directly augment the penalty for mixing requests to the reward function. Therefore, we set $\gamma - \tilde{\gamma}_e = 1$. For all experiments, we give equal weight to the impact on the prompt and decode phase. Therefore, α for equations subsection 5.2 and Equation 1 is set to 0.5. For workload-guided RL, we use the guidance mechanism from Equation 2. We set $\lambda_k = e^{-\beta_d k}$ (exponential decay over each episode) with $\beta_d = 0.5$, and the guided discount factor for training γ as $\hat{\gamma} = (1 - e^{-\beta_d k})\gamma$.

End-to-end latency. We evaluate our approaches by conducting 20 episodes, each comprising 2,000 requests with distinct characteristics. As illustrated in Figure 1b, our methods outperform the Round-Robin approach in terms of end-to-end latency for servicing all requests. On average, Baseline RL surpasses Round Robin by 7.53 seconds (4.35%). Incorporating the workload-aware penalty into the reward function enhances this advantage over Round Robin to 13.50 seconds (7.79%),

and utilizing the penalty as heuristic guidance for the RL agent further improves the advantage to 19.18 seconds (11.43%). Adding workload awareness to baseline RL helps to reduce the number of requests queuing at each model instance due to the adverse effect of mixing requests of distinct characteristics. However, such heuristics should be employed as a warm start and should be weaned down as the agent collects more information about the environment.

Additional Baselines. We further evaluate state-of-the-art heuristic algorithms used for the general purpose workloads against the proposed approach. In addition to Round Robin and the Lightweight Heuristic algorithm discussed above, we evaluated three more algorithms: (i) Join Shortest Queue, (ii) Maximum Capacity Usage and (iii) Min-Min Algorithm. Detailed explanation of these algorithms are attached in the appendix. We find that these algorithms are only marginally able to outperform round robin by (i) 0.46%, (ii) 2.60% and (iii) 1.50% in terms of end-to-end latency. The results are intuitive as classical heuristics do not translate well for LLM workloads due to their unique nature due to the auto-regressive nature of LLMs and the distinct characteristics of prefill and decode phases. Due to this, we provide further results in comparison to Round Robin only.

TTFT and TBT. All RL-based approaches improve upon the Round-robin router in terms of average TTFT (Figure 1c). The improvement is significant as the number of accumulated requests increases over time. Baseline RL effectively halves the TTFT for late-arriving requests by retaining them at the router and finding a better assignment than the round-robin approach, which immediately routes requests to a LLM instance. Incorporating the workload-aware penalty further enhances these decisions, though not optimally, as it dilutes the urgency to complete requests promptly and introduce constant bias throughout. The best performance is observed when workload awareness is employed as a heuristic guidance mechanism (Workload guided RL). We see similar patterns in the TBT of requests, as illustrated in Figure 5a, where Workload Aware and Workload Guided RL select more optimal model instances, mitigating spikes in the TBT of existing requests. Round-Robin performs better initially in terms of average TBT but the value increases over time as more requests with different characteristics accumulate. Baseline RL shows an increase in average TBT of around 20 seconds because the agent only optimizes for end-to-end latency and may end up adding requests with distinct characteristics to the same LLM instance, leading to higher TBT values. Although the average distribution of TBT across these methods is roughly similar, as shown in Figure 5b, workload awareness effectively reduces the number of outliers and the variance of the distribution.

Queuing of Requests at Router and Model Instance. Figure 5c illustrates the average length of the waiting queue at the model instances. While Baseline RL exhibits a shorter average waiting time of 0.59 seconds at the router, the requests get preempted at the model instances and accumulate substantial delays. This approach is suboptimal since postponing the routing decision could have resulted in better model instance getting assigned and resulted in faster processing of the request. In contrast, Workload Aware RL, with an average router wait time of 4.41 seconds, addresses this issue by incorporating a penalty based on the workload. Workload Guided RL further refines this strategy by utilizing the penalty as a guidance mechanism, resulting in an average router wait time of 2.05 seconds and improved overall performance.

Scalability Experiment. To further test the scalability of our approach, we test our methods with eight model instances. We increased the number of requests processed to 4000 and the request arrival rate to 40/s in order to remain consistency with previous experiments. In order to scale our approach, we needed to increase the parameters in our neural network. Our methods outperform the Round-Robin approach in this set up as well. On average, Baseline RL, Workload Aware RL and Workload Guided RL outperform Round Robin by 5.84%, 6.64% and 11.62% respectively.

7 Limitations and Conclusion

Conclusion. We propose a heuristic-guided Reinforcement Learning (RL) based router to efficiently schedule requests across LLM instances. Our approach introduces and models the novel notion of performance impact resulting from serving workloads with distinct characteristics concurrently. Incorporating prior knowledge on mixing workloads with distinct characteristics and their related adverse effects into the router gives improvements in overall end-to-end latency over current approaches. Our formulation is generalized enough to also improve over request-level metrics such as Time-To-First-Token (TTFT) and Time-Between-Two-Tokens (TBT).

Limitations. Due to resource constraints, we performed the experiments on the V100 and Llama 2 7B models. However, the current framework can be used to optimize routing for other hardware such as A100 or H100 by replicating the experiments and benchmarking. Also, our work currently focuses on First-Come-First-Served (FCFS) routing of requests. However, requests coming from different sources have varying urgency, which should be taken into account in future works.

References

- Daniel Adiwardana, Minh-Thang Luong, David R So, Jamie Hall, Noah Fiedel, Romal Thoppilan, Zi Yang, Apoorv Kulshreshtha, Gaurav Nemade, Yifeng Lu, et al. Towards a human-like open-domain chatbot. *arXiv preprint arXiv:2001.09977*, 2020.
- Amey Agrawal, Ashish Panwar, Jayashree Mohan, Nipun Kwatra, Bhargav S Gulavani, and Ramachandran Ramjee. Sarathi: Efficient llm inference by piggybacking decodes with chunked prefills. *arXiv preprint arXiv:2308.16369*, 2023.
- Amey Agrawal, Nitin Kedia, Ashish Panwar, Jayashree Mohan, Nipun Kwatra, Bhargav S. Gulavani, Alexey Tumanov, and Ramachandran Ramjee. Taming throughput-latency tradeoff in llm inference with sarathi-serve, 2024.
- Mark Chen, Jerry Tworek, Heewoo Jun, Qiming Yuan, Henrique Ponde de Oliveira Pinto, Jared Kaplan, Harri Edwards, Yuri Burda, Nicholas Joseph, Greg Brockman, et al. Evaluating large language models trained on code. *arXiv preprint arXiv:2107.03374*, 2021.
- Ching-An Cheng, Andrey Kolobov, and Adith Swaminathan. Heuristic-guided reinforcement learning. *Advances in Neural Information Processing Systems*, 34:13550–13563, 2021.
- Tri Dao, Dan Fu, Stefano Ermon, Atri Rudra, and Christopher Ré. Flashattention: Fast and memory-efficient exact attention with io-awareness. *Advances in Neural Information Processing Systems*, 35:16344–16359, 2022.
- Leon Derczynski, Eric Nichols, Marieke van Erp, and Nut Limsopatham. Results of the WNUT2017 shared task on novel and emerging entity recognition. In *Proceedings of the 3rd Workshop on Noisy User-generated Text*, pages 140–147, Copenhagen, Denmark, September 2017. Association for Computational Linguistics. doi: 10.18653/v1/W17-4418. URL <https://www.aclweb.org/anthology/W17-4418>.
- Angela Fan, Yacine Jernite, Ethan Perez, David Grangier, Jason Weston, and Michael Auli. ELI5: long form question answering. In Anna Korhonen, David R. Traum, and Lluís Màrquez, editors, *Proceedings of the 57th Conference of the Association for Computational Linguistics, ACL 2019, Florence, Italy, July 28- August 2, 2019, Volume 1: Long Papers*, pages 3558–3567. Association for Computational Linguistics, 2019. doi: 10.18653/v1/p19-1346. URL <https://doi.org/10.18653/v1/p19-1346>.
- Google. Vertex ai. <https://cloud.google.com/vertex-ai>.
- HuggingFace. Hugging face inference api. <https://huggingface.co/inference-api>.
- Neharika Jali, Guannan Qu, Weina Wang, and Gauri Joshi. Efficient reinforcement learning for routing jobs in heterogeneous queueing systems. *arXiv preprint arXiv:2402.01147*, 2024.
- Archit Patke¹ Dhmath Reddy¹ Saurabh Jha, Christian Pinto³ Haoran Qiu, Shengkun Cui¹ Chandra Narayanaswami² Zbigniew Kalbarczyk, and Ravishankar Iyer. Qlm: Queue management for large language model serving.
- Siddharth Jha, Coleman Hooper, Xiaoxuan Liu, Sehoon Kim, and Kurt Keutzer. Learned best-effort llm serving. *arXiv preprint arXiv:2401.07886*, 2024.
- Yunho Jin, Chun-Feng Wu, David Brooks, and Gu-Yeon Wei. $\$^{\wedge}3$: Increasing GPU utilization during generative inference for higher throughput. In *Thirty-seventh Conference on Neural Information Processing Systems*, 2023. URL <https://openreview.net/forum?id=zUYfbdN11m>.

- Woosuk Kwon, Zhuohan Li, Siyuan Zhuang, Ying Sheng, Lianmin Zheng, Cody Hao Yu, Joseph E. Gonzalez, Hao Zhang, and Ion Stoica. Efficient memory management for large language model serving with pagedattention. In *Proceedings of the ACM SIGOPS 29th Symposium on Operating Systems Principles*, 2023.
- Jiamin Li, Le Xu, Hong Xu, and Aditya Akella. Blockllm: Multi-tenant finer-grained serving for large language models. *arXiv preprint arXiv:2404.18322*, 2024.
- Bin Lin, Tao Peng, Chen Zhang, Minmin Sun, Lanbo Li, Hanyu Zhao, Wencong Xiao, Qi Xu, Xiafei Qiu, Shen Li, et al. Infinite-llm: Efficient llm service for long context with distattention and distributed kvcache. *arXiv preprint arXiv:2401.02669*, 2024.
- Jiachen Liu, Zhiyu Wu, Jae-Won Chung, Fan Lai, Myungjin Lee, and Mosharaf Chowdhury. Andes: Defining and enhancing quality-of-experience in llm-based text streaming services. *arXiv preprint arXiv:2404.16283*, 2024.
- Andrew L. Maas, Raymond E. Daly, Peter T. Pham, Dan Huang, Andrew Y. Ng, and Christopher Potts. Learning word vectors for sentiment analysis. In *Proceedings of the 49th Annual Meeting of the Association for Computational Linguistics: Human Language Technologies*, pages 142–150, Portland, Oregon, USA, June 2011. Association for Computational Linguistics. URL <http://www.aclweb.org/anthology/P11-1015>.
- Daniel Mendoza, Francisco Romero, and Caroline Trippel. Model selection for latency-critical inference serving. In *Proceedings of the Nineteenth European Conference on Computer Systems*, pages 1016–1038, 2024.
- Microsoft. Azure ai studio. <https://ai.azure.com/>.
- OpenAI. Openai platform. <https://platform.openai.com/overview>.
- Pratyush Patel, Esha Choukse, Chaojie Zhang, Íñigo Goiri, Aashaka Shah, Saeed Maleki, and Ricardo Bianchini. Splitwise: Efficient generative llm inference using phase splitting, 2023.
- Ramya Prabhu, Ajay Nayak, Jayashree Mohan, Ramachandran Ramjee, and Ashish Panwar. vattention: Dynamic memory management for serving llms without pagedattention. *arXiv preprint arXiv:2405.04437*, 2024.
- Haoran Qiu, Weichao Mao, Archit Patke, Shengkun Cui, Saurabh Jha, Chen Wang, Hubertus Franke, Zbigniew T Kalbarczyk, Tamer Başar, and Ravishankar K Iyer. Efficient interactive llm serving with proxy model-based sequence length prediction. *arXiv preprint arXiv:2404.08509*, 2024.
- Pranav Rajpurkar, Jian Zhang, Konstantin Lopyrev, and Percy Liang. SQuAD: 100,000+ questions for machine comprehension of text. In Jian Su, Kevin Duh, and Xavier Carreras, editors, *Proceedings of the 2016 Conference on Empirical Methods in Natural Language Processing*, pages 2383–2392, Austin, Texas, November 2016. Association for Computational Linguistics. doi: 10.18653/v1/D16-1264. URL <https://aclanthology.org/D16-1264>.
- Stephen Roller, Emily Dinan, Naman Goyal, Da Ju, Mary Williamson, Yinhan Liu, Jing Xu, Myle Ott, Kurt Shuster, Eric M Smith, et al. Recipes for building an open-domain chatbot. *arXiv preprint arXiv:2004.13637*, 2020.
- Benjamin Spector and Chris Re. Accelerating llm inference with staged speculative decoding. *arXiv preprint arXiv:2308.04623*, 2023.
- Alessandro Staffolani, Victor-Alexandru Darvari, Paolo Bellavista, and Mirco Musolesi. Rlq: Workload allocation with reinforcement learning in distributed queues. *IEEE Transactions on Parallel and Distributed Systems*, 34(3):856–868, 2023.
- Jörg Tiedemann. Parallel data, tools and interfaces in OPUS. In Nicoletta Calzolari, Khalid Choukri, Thierry Declerck, Mehmet Uğur Doğan, Bente Maegaard, Joseph Mariani, Asuncion Moreno, Jan Odijk, and Stelios Piperidis, editors, *Proceedings of the Eighth International Conference on Language Resources and Evaluation (LREC'12)*, pages 2214–2218, Istanbul, Turkey, May 2012. European Language Resources Association (ELRA). URL http://www.lrec-conf.org/proceedings/lrec2012/pdf/463_Paper.pdf.

Hugo Touvron, Louis Martin, Kevin Stone, Peter Albert, Amjad Almahairi, Yasmine Babaei, Nikolay Bashlykov, Soumya Batra, Prajjwal Bhargava, Shruti Bhosale, Dan Bikel, Lukas Blecher, Cristian Canton Ferrer, Moya Chen, Guillem Cucurull, David Esiobu, Jude Fernandes, Jeremy Fu, Wenyin Fu, Brian Fuller, Cynthia Gao, Vedanuj Goswami, Naman Goyal, Anthony Hartshorn, Saghar Hosseini, Rui Hou, Hakan Inan, Marcin Kardas, Viktor Kerkez, Madian Khabsa, Isabel Kloumann, Artem Korenev, Punit Singh Koura, Marie-Anne Lachaux, Thibaut Lavril, Jenya Lee, Diana Liskovich, Yinghai Lu, Yuning Mao, Xavier Martinet, Todor Mihaylov, Pushkar Mishra, Igor Molybog, Yixin Nie, Andrew Poulton, Jeremy Reizenstein, Rashi Rungta, Kalyan Saladi, Alan Schelten, Ruan Silva, Eric Michael Smith, Ranjan Subramanian, Xiaoqing Ellen Tan, Binh Tang, Ross Taylor, Adina Williams, Jian Xiang Kuan, Puxin Xu, Zheng Yan, Iliyan Zarov, Yuchen Zhang, Angela Fan, Melanie Kambadur, Sharan Narang, Aurelien Rodriguez, Robert Stojnic, Sergey Edunov, and Thomas Scialom. Llama 2: Open foundation and fine-tuned chat models, 2023.

Bingyang Wu, Yinmin Zhong, Zili Zhang, Gang Huang, Xuanzhe Liu, and Xin Jin. Fast distributed inference serving for large language models. *arXiv preprint arXiv:2305.05920*, 2023.

Gyeong-In Yu, Joo Seong Jeong, Geon-Woo Kim, Soojeong Kim, and Byung-Gon Chun. Orca: A distributed serving system for Transformer-Based generative models. In *16th USENIX Symposium on Operating Systems Design and Implementation (OSDI 22)*, pages 521–538, Carlsbad, CA, July 2022. USENIX Association. ISBN 978-1-939133-28-1. URL <https://www.usenix.org/conference/osdi22/presentation/yu>.

Zhenyu Zhang, Ying Sheng, Tianyi Zhou, Tianlong Chen, Lianmin Zheng, Ruisi Cai, Zhao Song, Yuandong Tian, Christopher Ré, Clark Barrett, et al. H2o: Heavy-hitter oracle for efficient generative inference of large language models. *Advances in Neural Information Processing Systems*, 36, 2024.

Yinmin Zhong, Shengyu Liu, Junda Chen, Jianbo Hu, Yibo Zhu, Xuanzhe Liu, Xin Jin, and Hao Zhang. Distserve: Disaggregating prefill and decoding for goodput-optimized large language model serving. *arXiv preprint arXiv:2401.09670*, 2024.

A Appendix / supplemental material

A.1 Batching and Routing Algorithms

All the batching algorithms are non-preemptive in nature, meaning that once the processing of a request has started, it is prioritized over requests which have not. Next, we discuss different batching and routing algorithms defined in section 4.

Batching: Bin Packing Algorithm. When a new request’s processing can be started, we select the largest request that can fit into the memory available. Ties are broken by FCFS.

Batching: Least Work Left. Among the requests available, we select the request with the smallest number of decode tokens.

Batching: FCFS. The request which arrives first is processed first.

Routing: Dedicated Small-Large. For the two LLM model instances, we dedicate one instance for servicing only the heavy-decode requests while the other model instance services only the light-decode requests.

Routing: Round Robin. Each of the two model is user alternatively by the router to send requests to.

Routing: Decode Balancer We assume that the total number of output tokens is known beforehand for the request and we balance the sum of decode tokens on both the model instances.

A.2 Additional Baselines

We implemented three baselines other than Round Robin and the Light-weight Heuristic:

A.2.1 Join Shortest Queue

Each arriving request is routed to the model with the least number of prompt and decode tokens yet to be processed.

A.2.2 Maximum Capacity Usage

Request at the front of the queue is routed to the model with the maximum capacity available, given that it can process this particular request, at intervals of one second.

A.2.3 Min-Min Algorithm

We implemented the classical Min-min algorithm, using the number of prompt tokens and the upper bound of the predicted decode token buckets to calculate the time for finishing each job. Since we have homogenous model instances, this strategy becomes similar to shortest job first.

A.3 Details of Dataset

From each dataset, we take the subset of prompts that have a maximum prompt length of 1000 tokens.

A.3.1 Prompts

For each task, the prompt is created in the following manner:

Sentiment Analysis (IMDb dataset) For each review in the dataset, we randomly select one of the following sentences and add it to the review:

1. "Based on this review, judge if the user liked this movie or not?"
2. "Please identify if the review is positive or negative?"
3. "Based on this review, should we recommend this movie to other users with similar tastes?"

We add these tasks either at the beginning or at the end of the prompts, again randomly.

QnA (Eli5 Reddit subset) We pick the question in the title as it is and provide it as the prompt to the LLM.

Entity Recognition (WNUT dataset) We add the suffix "Can you identify the <entity> mentioned in the above sentence?" where <entity> is selected randomly from "person", "place", and "object".

In context QnA (SQuAD dataset) We add the question as well as the four options of the answer to the prompt and ask the LLM to select the correct option and provide reasoning with it as well.

Translation (Books dataset) We provide the text and add the phrase "Please translate this text into <language>" either at the start or at the end of the text. <language> is selected from the ones provided in the dataset itself.

A.3.2 Task Hints

For providing a hint of the task to the model, we add the phrase "This is a <task> task" at the end of each prompt before providing it to the classifier.

A.4 Prompt-Decode Distribution

Figure 6 shows the distribution of prompts and decode tokens across the different datasets we mixed. We can clearly see the different distributions each dataset has. Prompts from Eli-5 Reddit subset are shorter in length and have longer responses than the rest of the dataset, while the IMDb distribution on the other hand has longer prompt lengths and shorter responses. Such a varied distribution contributes to the low accuracy of the current SOTA model by Jin et al. [2023].

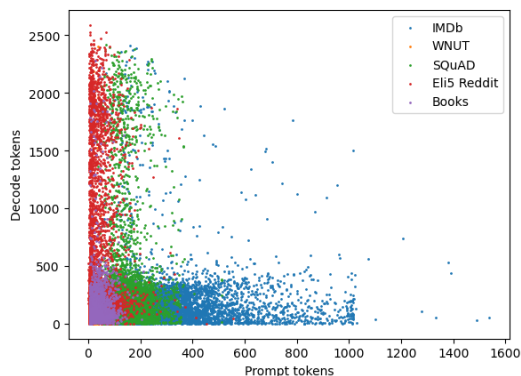


Figure 6: Prompt decode distribution for our dataset with responses generated from Llama 2 7B model.

A.5 Training details of the output length predictor

We had a total of 31329 samples in our mixed dataset, from which we had an 80:20 train-test split. We had a train time accuracy of 81% after performing 6 epochs of fine-tuning with the entire training set.

A.6 Task Predictability

We predict the task of a prompt sampled from our dataset described in section 4 using DistillBERT, the same methodology we use to predict their output length bucket as discussed in subsection 5.1. We observe an accuracy of 93.79%.

This allows us to proceed safely with the assumption that we can provide task type as part of the prompt to the output length predictor.

A.7 Licenses

1. WNUT Dataset: CC-by-4.0
2. SQuAD dataset: CC-by-SA-4.0
3. vLLM: Apache-2.0

A.8 Details of RL training

For our experiments, we use 4 LLM model instances to route among. This results in our state space having 27 dimensions (6 for each model instance and 4 for the request queue at the router). In order to bound our state space, we round the estimated capacity available at each model instance and the estimated completion time for the earliest request to two decimal places. We also upper bound the waiting queue length that we provide to the DQN to $4 \times (\max \text{ batch size}) = 4 \times 128 = 512$. We provide the DQN with 3 buckets: 0-256, 256-2048, ≥ 2048 .

A.8.1 Q-Learning

Q-Learning yields poor performance for our task due to the size of the state space. If we upper bound the total number of requests that can be present at a model instance to 150 (even though there can be infinitely many) and the prompt and decode length to 4096 (maximum content window of LLama-2 7B), each model instance can be in $150 \times 150 \times 100 \times (4096 \times 150 \times \text{grad}_2 \times 100) = 3.0405 \times 10^9$ different states. This would result in a total of $(3.0405 \times 10^9)^4 \times 512 \times 4096 \times 3 \approx 5 \times 10^{44}$. Even though we will never visit most of these states, the possible states that be visited are large enough to make Q-Learning infeasible.

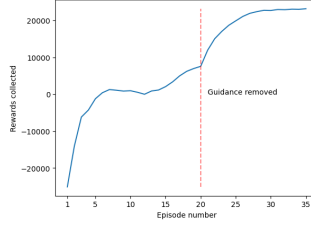


Figure 7: Training reward for workload guided RL

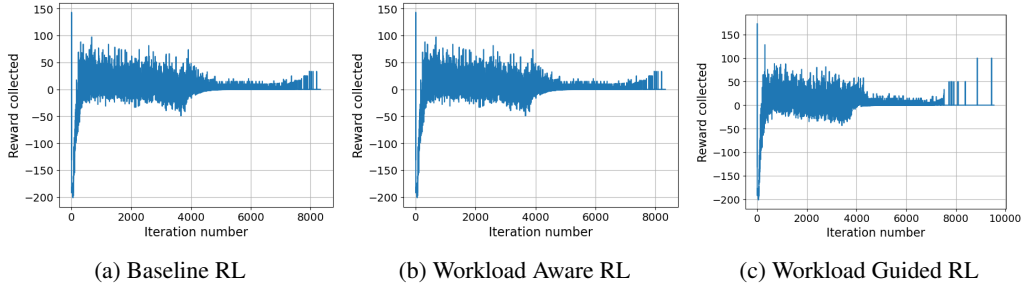


Figure 8: Rewards collected during testing for each strategy

A.8.2 Training Rewards

Figure 7 Shows the rewards collected during training of the RL model. We see that the guidance heuristic helps the agent converge. After episode 20, we no longer use explore with random actions and exploit this knowledge.

A.8.3 Double-DQN

We take a double DQN approach for our RL agent. We set the request completion reward to 60 and train our DQN with a batch size of 512. We use a neural network with layer sizes (27, 64), (64, 64), (64, 5) and ReLU activation function for layers 1 and 2.

Figure 8 shows the rewards collected by each strategy during testing. Requests stop arriving at iteration number 4000, after which, we see the rewards tend to positive values due to the high request completion reward.

A.9 Overhead of the router

For each decision, the router has to perform two additional steps in our approach: (i) inference from DistillBERT for output length bucket and (ii) inference from the neural network being used. The approach can parallelize these modules when the number of requests in the queue is large (and the request being routed has already been processed by the length predictor). (i) takes us 0.01 (on GPU) and 0.8 (on CPU) seconds per batch of size 64 and (ii) takes $< 10^6$ operations (within milliseconds) to process.